PACS photometer point spread function

Dieter Lutz

1 Summary

The PACS PV plan includes a broad range of observations aiming to characterise the PSF for a wide range of observing modes and source SEDs. The SED distinction is made because of the expected dependence of PSF on SED slope, which is due the wide filter bandpasses.

The quick version 0.3 of this note presents results derived from scanmap observations of the star α Tau in OD118, and of Vesta in OD160, both being 'hot' sources. A final PSF characterisation will have to be based on a wider set of observations and make use of calibrations and reduction steps currently not yet available, but the current set of results should be useful for many purposes. The associated PSF images are available on request.

The photometer PSF is characterised by

- A narrow core which is round in the blue bands but slightly elongated in spacecraft Z direction in red.
- A tri-lobe pattern seen at the several % level in all bands, most clearly in the blue with its strongest signal, and ascribed to imperfect mirror shape.
- Knotty structure at sub-percent level, clearly seen in blue and green.

For fast scans in normal and parallel mode, this PSF structure is smeared by detector time constants and data averaging.

The most prominent unusual effects are (1) a narrow and faint spike, extending in z direction. This spike is seen in blue and green and also indicated in red, and (2) a negative PSF feature in the scan direction of blue/green fast scans which is perhaps indicative of an undershooting of the signal after source passage.

At the faintest level of the blue psf there is an indication for the six-spoke diffraction pattern caused by the secondary mirror support.

2 Data reference sheet

OD	OBSID	Source	HSPOT name	sec
118	1342183538	αTau	Calibration_PVPhotSpatial_1-PVPhotSpatial_314D_StdScan_blumed_AlfTau_0001	
118	1342183539	αTau	Calibration_PVPhotSpatial_1-PVPhotSpatial_314D_StdScan_bluhigh_AlfTau_0001	
118	1342183540	αTau	Calibration_PVPhotSpatial_1-PVPhotSpatial_314D_StdScan_blulow_AlfTau_0001	
118	1342183541	αTau	Calibration_PVPhotSpatial_1-PVPhotSpatial_314D_StdScan_grnmed_AlfTau_0001	
118	1342183542	αTau	Calibration_PVPhotSpatial_1-PVPhotSpatial_314D_StdScan_grnhigh_AlfTau_0001	
118	1342183543	αTau	Calibration_PVPhotSpatial_1-PVPhotSpatial_314D_StdScan_grnlow_AlfTau_0001	
137	1342184486	Mars	Calibration_PVParStray_1-PVParStray_316A_TFOV_blu2dx2d_centre_Mars_OD137	
160	1342186132	Vesta	Calibration_PVPhotSpatial_1-PVPhotSpatial_314D_StdScan_grnlow_Vesta_0001	
160	1342186133	Vesta	Calibration_PVPhotSpatial_1-PVPhotSpatial_314D_StdScan_grnmed_Vesta_0001	
160	1342186134	Vesta	Calibration_PVPhotSpatial_1-PVPhotSpatial_314D_StdScan_grnhigh_Vesta_0001	
160	1342186135	Vesta	Calibration_PVPhotSpatial_1-PVPhotSpatial_314D_StdScan_blulow_Vesta_0001	
160	1342186136	Vesta	Calibration_PVPhotSpatial_1-PVPhotSpatial_314D_StdScan_blumed_Vesta_0001	
160	1342186137	Vesta	Calibration_PVPhotSpatial_1-PVPhotSpatial_314D_StdScan_bluhigh_Vesta_0001	
173	1342186639	Neptune	Calibration_PVPhotFlux_1-PVPhotFlux_321D_StdScan_045_pcal_blu_Neptune_0001	
173	1342186640	Neptune	Calibration_PVPhotFlux_1-PVPhotFlux_321D_StdScan_135_pcal_blu_Neptune_0001	
173	1342186641	Neptune	Calibration_PVPhotFlux_1-PVPhotFlux_321D_StdScan_045_pcal_grn_Neptune_0001	
173	1342186642	Neptune	Calibration_PVPhotFlux_1-PVPhotFlux_321D_StdScan_135_pcal_grn_Neptune_0001	

3 Description of observations

The dedicated PSF observations are scanmaps centered on the star α Tau or on the asteroid Vesta, using 15 scanlegs with 3 arcsec cross-scan separation. The orientation angle is 63 degree in the array frame, along the array diagonal. This pattern is overall providing source passages over many regions of the array and with good sub-pixel sampling.

The fluxes of αTau are about 14.0–6.9–2.7Jy at 70–100–160μm according to the PV plan PICC-MA-PL-001. The flux of Vesta during the OD160 observations was about 93–49–20Jy (T. Müller 26.10.2009)

Scanmaps of Mars and Neptune are used to investigate fainter PSF structures.

4 Analysis methods and dp scripts used

The reduction uses two main steps (1) determination of pointing corrections and (2) mapping.

Pointing corrections are determined in a first pass by comparing frame per frame the expected location of the source on the array (computed from pointing product info and PACS spatial calibration) with the measured position from a 2-d gaussian fit. Only frames for which the source was centered at least 1.5 pixels inside a matrix were kept. The corrections derived were then used in the second pass processing to adjust the input RA, DEC coordinates of each frame to achieve consistency between expected and actual centroid on the frame. Given instantaneous S/N in the respective filters, corrections were derived from the blue/green data and applied also to the red data, considering the time shift of the frame indices in each camera.

The second pass is a highpass-filtered scanmap production making use of the corrected pointing.

- Calblock related steps and drift correction were bypassed.
- 'Glitches' found by MMT deglitching within about 10 arcsec from the source were explicitly not deglitched to avoid affecting the PSF core. Coverage maps were checked and had no dips at the source position any more. For Vesta this radius had to be enlarged especially for the fast scan, and some glitches surviving this automatic procedure can be seen in the psf maps. No attempt was made to manually remove them.
- A region with 35 arcsec (α Tau) or 60 arcsec (Vesta) radius centered on the source was masked in the highpass filtering to suppress the familiar filtering residues on both sides of the bright source. A highpass filter radius of 100 arcsec on sky was used.
- All maps were projected on a 1 arcsec pixel grid with a map position angle based on the spacecraft PA, so that the image axes align with the spacecraft y,z directions.
- The Vesta-based psfs were explicitly corrected to "Daophot"-background 0 in an annular aperture of radius 61-70arcsec, for consistency with the encircled energy fraction curve shown below.

All the data were taken in standard scan mode but we simulate the PSF for parallel mode 60arcsec/sec, which is averaging 8 40Hz samples. This is done by averaging the fluxes and coordinates of 2 consecutive frames of our 60arcsec/sec 4 40Hz sample averaged data.

The data for Vesta, a solar system object moving at 53arcsec/h at the time of the observations, were made amenable to the same processing by applying a suitable linear correction to the coordinates as a function of time.

Our reduction procedure has a number of implications on the derived PSF that are worth mentioning:

- PSFs measured in standard scanmap reductions will typically be wider, due to currently imperfect PACS spatial calibration, potential small synchronisation issues data/pointing and due to pointing jitter, all of which are tackled ad hoc by the recentering. The first factor may be reduced in the future with improving calibration while the last will always remain for faint source data to some level.
- These PSFs represent the convolution of the telescope PSF with the PACS pixel size - PRFs in Spitzer speak. The map pixel is small in comparison.
- Because of redundancy, results should be more robust to current incomplete knowledge of reduction steps like flatfield, dubious pixels, crosstalk etc. than chopped/nodded observations, but nevertheless subject to update.
- For fast scan and parallel mode, there could be subtle but basic differences between the PSFs derived here from several back and forth scans and using recentering, to PSF from single pass unidirectional scans, because of the effects of detector time response.
- By definition of the recentering step, the PSFs will not include ghost related features arising while the source was off the array (e.g., a possible effect of the 'blue streaks' seen for sources just outside the array corner in FM-ILT).

Maps of the bright sources Mars and Neptune were analysed in a quicker and more simple way, not trying to recenter or correct for proper motion. While masking and large filter widths were used to preserve extended

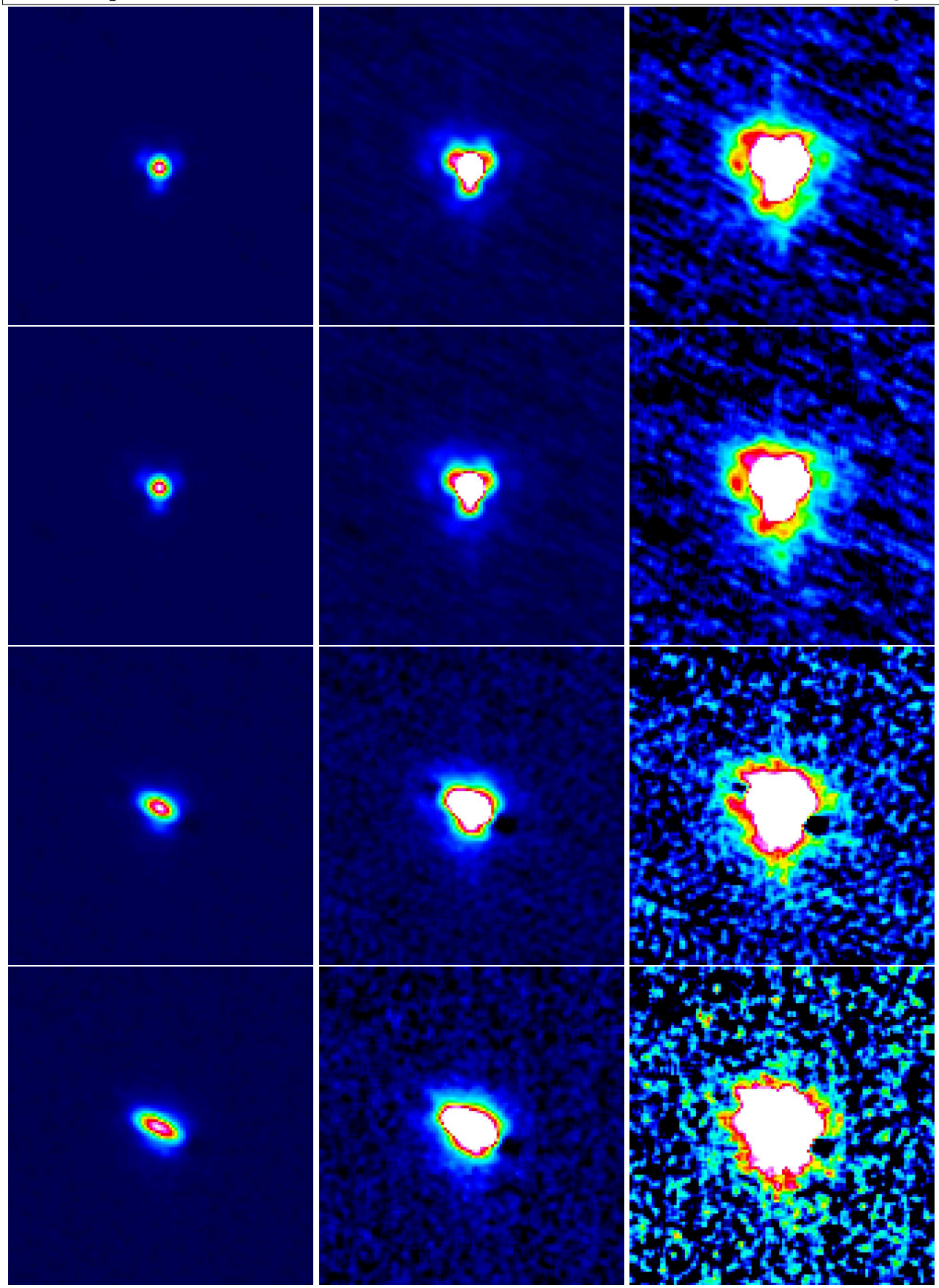

Figure 1: Blue PSF from α Tau data, from left to right linearly scaled to peak, 10% of peak, and 1% of peak. From top to bottom scanspeed 10, 20, 60 arcsec/sec and (simulated) parallel mode at 60 arcsec/sec. Spacecraft Z is on top as if PA=0, scan angle 63deg in array coordinates.

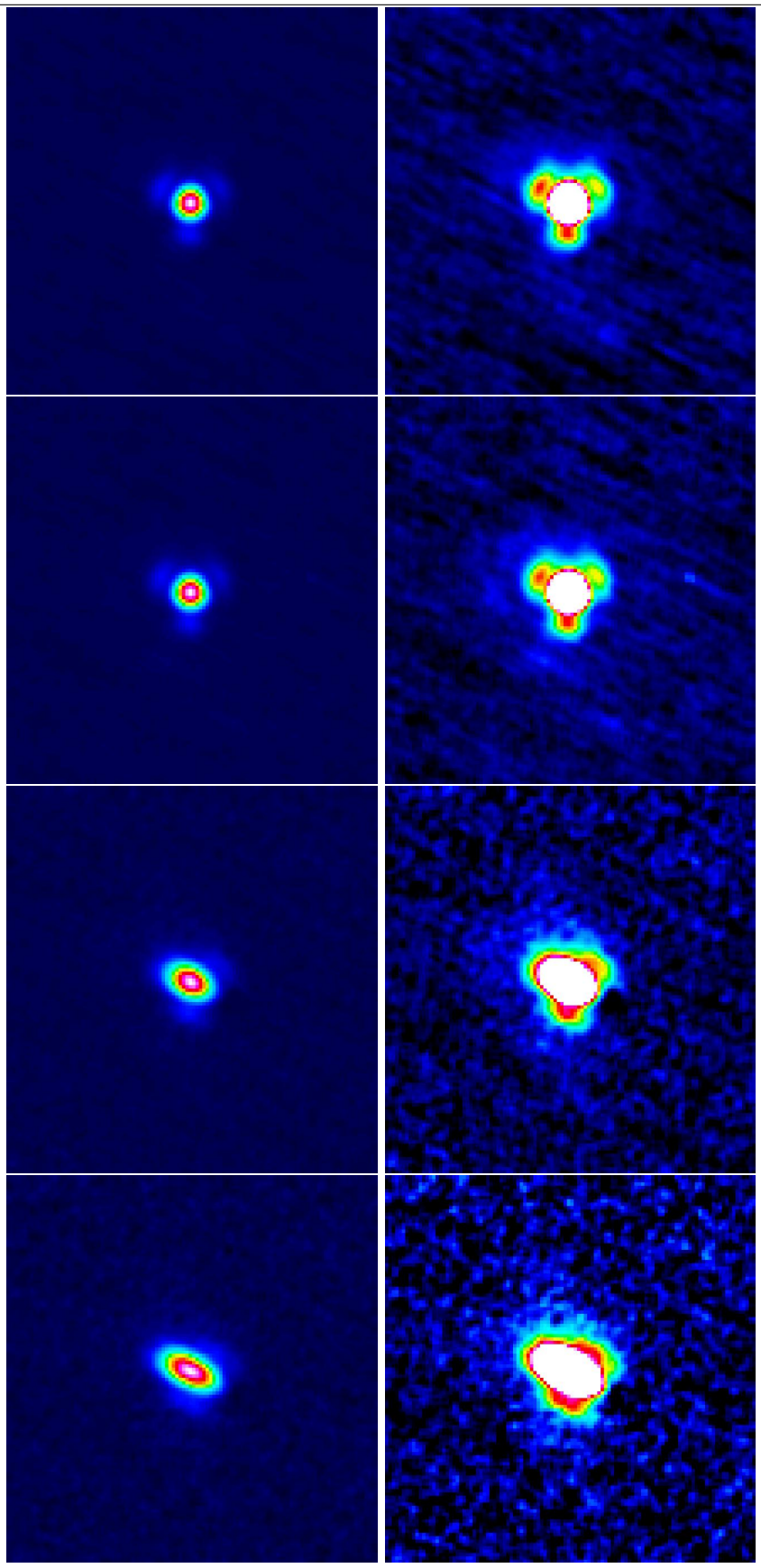

Figure 2: Green PSF from α Tau data, from left to right linearly scaled to peak and 10% of peak. From top to bottom scanspeed 10, 20, 60 arcsec/sec and (simulated) parallel mode at 60 arcsec/sec.

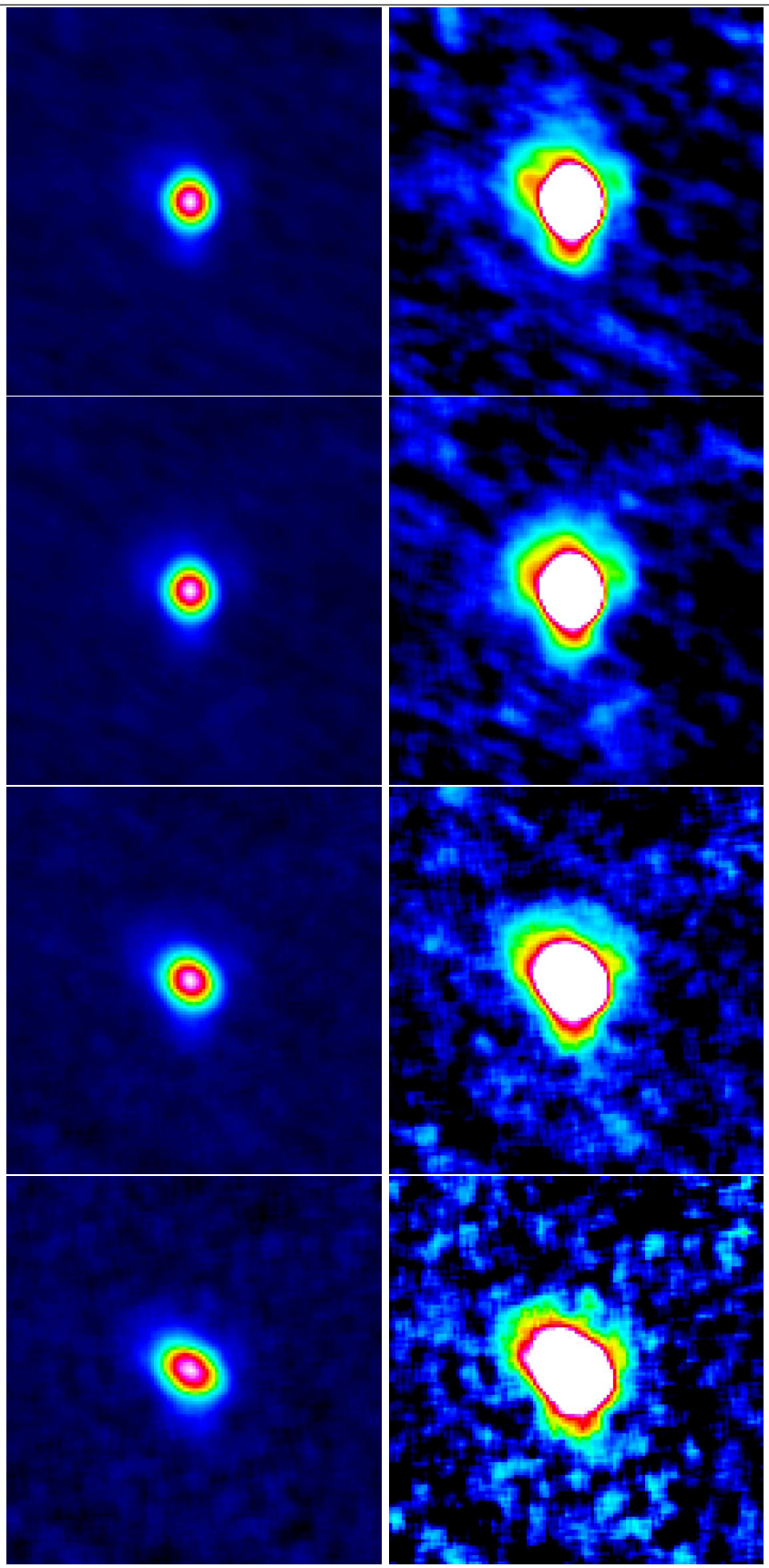

Figure 3: Red PSF from α Tau data, from left to right linearly scaled to peak and 10% of peak. From top to bottom scanspeed 10, 20, 60 arcsec/sec and (simulated) parallel mode at 60 arcsec/sec.

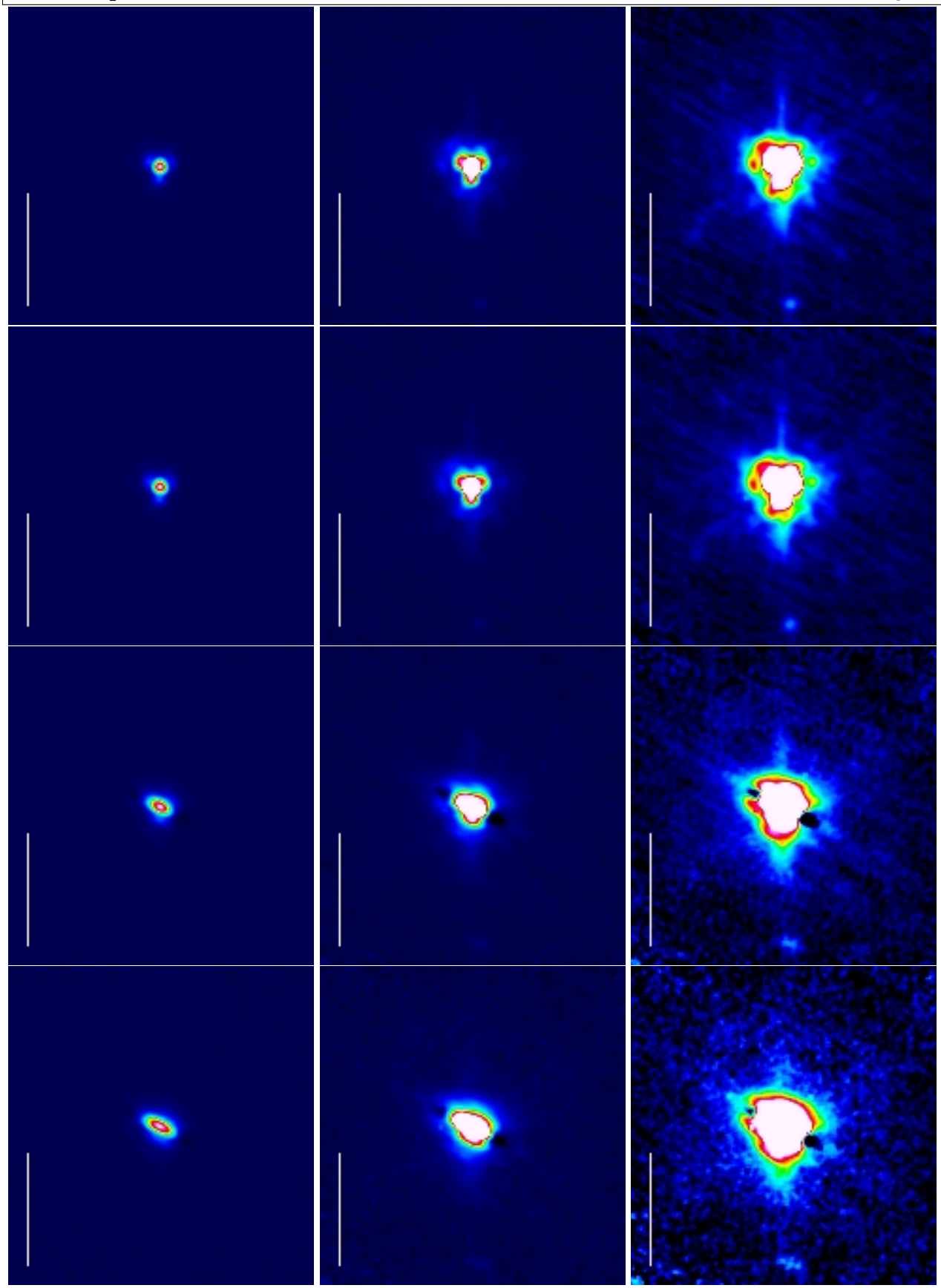

Figure 4: Blue PSF from Vesta data, from left to right linearly scaled to peak, 10% of peak, and 1% of peak. From top to bottom scanspeed 10, 20, 60 arcsec/sec and (simulated) parallel mode at 60 arcsec/sec. Spacecraft Z is on top as if PA=0, scan angle 63deg in array coordinates. The scale bar indicates 60arcsec.

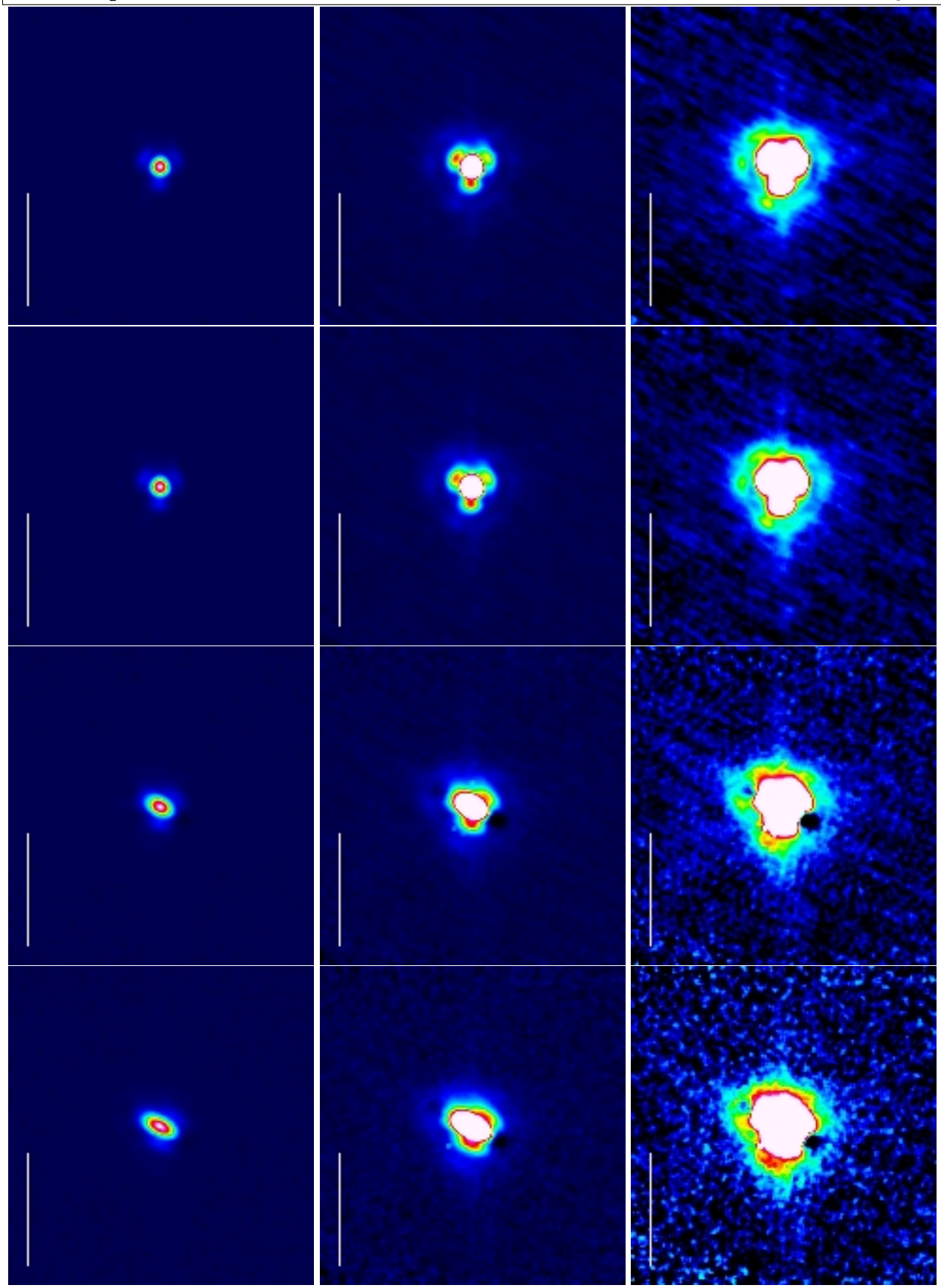

Figure 5: Green PSF from Vesta data, from left to right linearly scaled to peak and 10% of peak. From top to bottom scanspeed 10, 20, 60 arcsec/sec and (simulated) parallel mode at 60 arcsec/sec. The scale bar indicates 60arcsec.

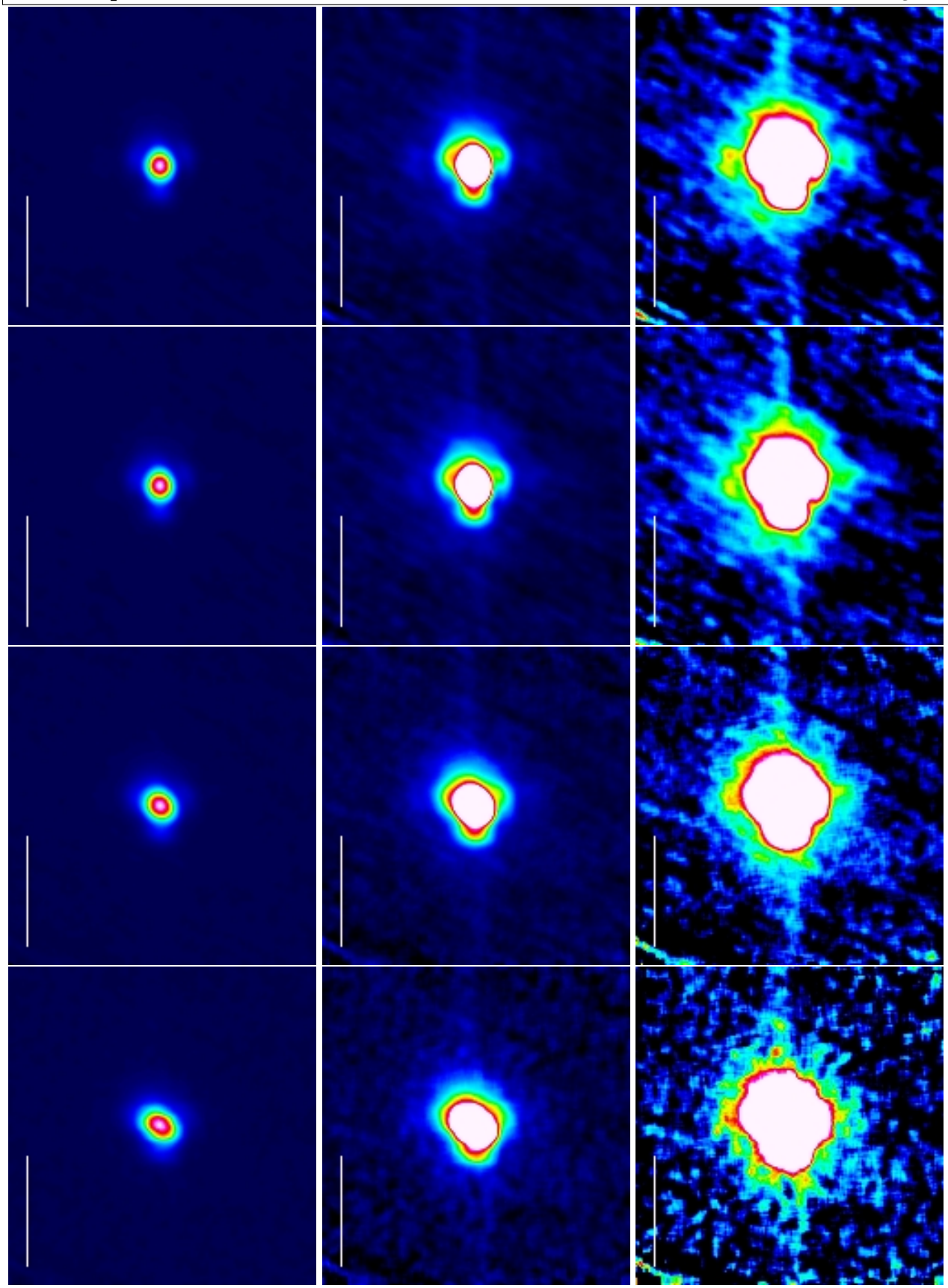

Figure 6: Red PSF from Vesta data, from left to right linearly scaled to peak and 10% of peak. From top to bottom scanspeed 10, 20, 60 arcsec/sec and (simulated) parallel mode at 60 arcsec/sec. The scale bar indicates 60arcsec.

structure, and some steps were made to reduce deglitching artefacts, it is clear that the maps shown are far from ideal inparticular with respect to deglitching.

5 Results

Figures 1 to 3 show the resulting α Tau PSF images at different linear stretches 0.05–1, 0.005-0.1 and where possible 0.0005-0.01 times the PSF peak. Figures 4 to 6 provide the equivalent information for the higher S/N Vesta data. The linear noise structures in scan direction are a consequence of the fairly generous highpass filter width used. It should be noted that at the given noise level, background sources start to be detected and are in fact seen outside the image panels shown. While formal proof that any faint feature seen is not due to a background object or real structure near α Tau or Vesta will need confirmation on several independent sources, we proceed here with the assumption that structures above the noise are PSF features. The good agreement between the two datasets from different targets supports this.

Table 1 summarizes results from fitting 2-dimensional gaussian to the full PSF including wings. While such gaussian fits may not be an optimal representation of the PSF they allow for quick comparison with mapping results. The PSF width in blue for slow scan is similar to first results seen in single frame staring data, giving confidence that the recentering/mapping procedure recovers the actual PACS PSF. The agreement between the widths measured from the two datasets is very good.

5.1 PSF morphology

In all three bands the PSF core is surrounded by a tri-lobe pattern at the level of up to 10% (in blue) of the PSF peak. Ongoing optical modelling by N.Geis attempts to reproduce this with surface properties of the main mirror which are reflecting among other things the 120 degree symmetry of the secondary mirror suspensions. In all three bands, the top-right of the three lobes is weakest.

The next fainter level of PSF structures is again not a clear diffraction ring but a knotty pattern at the % level and below. It is clearly seen in blue and well confirmed in the 10 vs. 20 arcsec/sec data. A similar pattern is seen in green but with less detail at current S/N.

The blue data show a weak spike in roughly vertical (spacecraft z) direction, perhaps similar to a spike seen in ILT data (FM report figure 1.124). The spike is clearly confirmed in green and perhaps also in red. Roughly 70arcsec towards the -z direction, a bright spot is superposed on this spike, clearly seen in blue and weakly in green. Neptune observations (see below) confirm this feature.

The fast scan blue/green PSF shows a region going to below zero, to a level of about -1% of the peak. Its origin is not understood, and undershooting of the signal after a short exposure to a bright signal would be needed to create it. It is unclear to which extent this effect is (non)linear. A test reduction using a huge highpass filter width and avoiding deglitching reproduced the effect.

At slow scanspeed, the PSF fits are roughly round for blue and green but vertically elongated in the red, this elongation is seen in the PSF core and not just an effect of wings or lobes. A slight elongation in same direction

was seen in ILT but cannot be compared quantitatively given the properties of the ILT setup plus its use of somewhat extended holes.

Comparing results for the slow scanspeeds 10 and 20 arcsec/sec, the PSFs are very similar in all bands. Fast scan and in particular parallel mode with 8-sample averaging show significant elongation in scan direction, as expected. The detailed PSF pattern for fast scan will depend on the relative orientation of scan direction and the tri-lobe pattern, the PSFs shown here can give only examples for the given scan direction relative to the array.

Band	Speed arcsec/sec	FWHM arcsec αTau OD118	PA deg	FWHM arcsec Vesta OD160	PA deg
Blue	10	5.26×5.61		5.24×5.61	
Blue	20	5.46×5.76		5.45×5.77	
Blue	60	5.75×9.00	62.0	5.72×9.11	61.7
Blue	60/para	5.86×12.16	63.0	5.83×12.12	62.4
Green	10	6.57×6.81		6.52×6.77	
Green	20	6.69×6.89		6.65×6.87	
Green	60	6.89×9.74	62.3	6.82×9.80	61.7
Green	60/para	6.98×12.70	63.0	6.91×12.60	62.5
Red	10	10.46×12.06	7.6	10.34×11.92	6.2
Red	20	10.65×12.13	9.3	10.50×12.02	9.2
Red	60	11.31×13.32	40.9	11.33×13.29	41.3
Red	60/para	11.64×15.65	53.4	11.60×15.42	53.4

Table 1: Results of fitting 2-dimensional gaussians to the PSF for both αTau and Vesta. Note these are fits to the full PSF including the lobes/wings. Position angles (east of north) are listed only for beams with clearly elongated core. Scan angle is 63deg for these observations.

6 Encircled energy diagrams

The PSFs derived from the OD160 Vesta data are of sufficient S/N to derive encircled energy fractions for the 3 bands as a function of the radius of a circular aperture (Fig. 7). The EEF fraction shown is normalized to the signal in aperture radius 60arcsec, with background subtraction done in an annulus between radius 61 and 70 arcsec.

7 PSF morphology at faint levels

αTau and Vesta are selected to be bona fide PSF sources: Pointlike, and no surrounding FIR structure. They are still faint enough to not induce significant nonlinearities in the bolometer response. Conversely, they are not bright enough to reveal the faintest PSF detail, and integrating longer would pose a danger of detecting additional fainter background sources.

For this reason, scanmaps of Mars (OD137, parallel mode) and Neptune (OD173, scanmap) were inspected for faint PSF details. ***It should be noted that at the current state of pacs reduction, details of (masked) filtering, deglitching, flatfielding, crosstalk are or may still be present at noticeable levels in the***

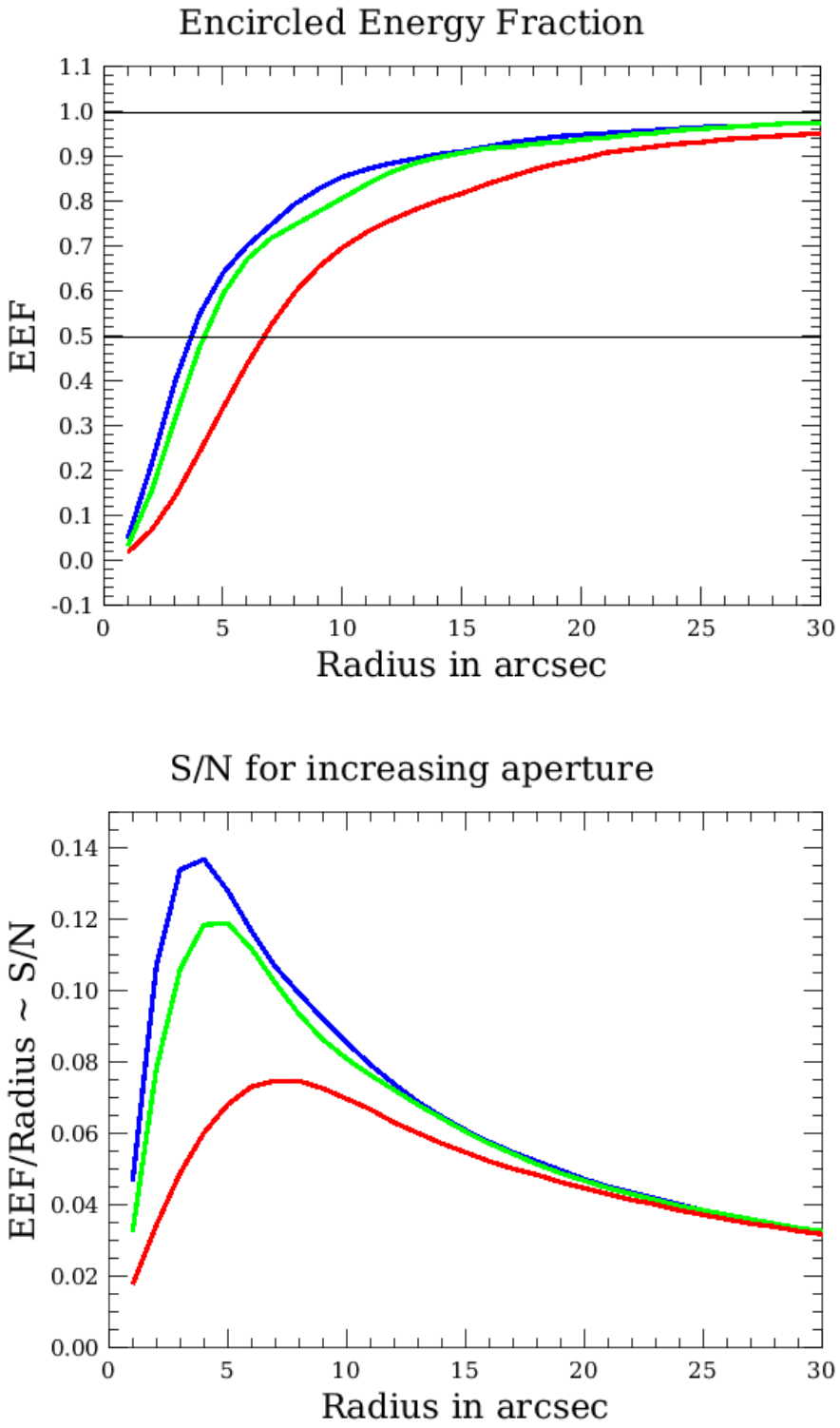

Figure 7: Top: Encircled energy fraction as a function of circular aperture radius for the three bands. Derived from slow scan OD160 Vesta data.The EEF fraction shown is normalized to the signal in aperture radius 60arcsec, with background subtraction done in an annulus between radius 61 and 70 arcsec The bottom panel shows the corresponding S/N curve under the assumption that noise scales linearly with aperture radius. Note that this assumption is not met for scanmaps with 1/f noise.

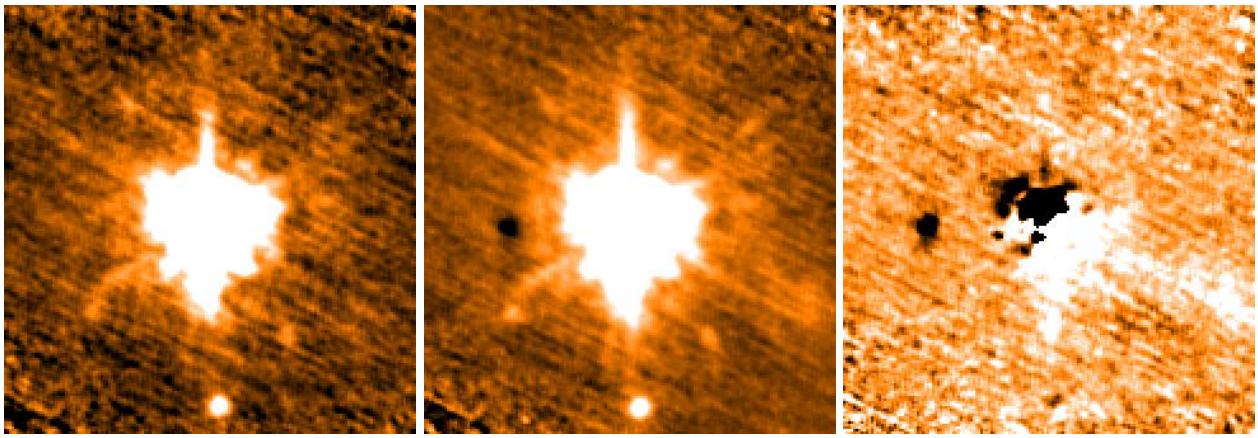

Figure 8: Illustration how mapped area and processing may affect the retrieved PSF. Left: Vesta as processed for the PSF analysis, Middle: Normal processing from full AOR and with relaxed deglitching, Right: Difference image.

maps shown. Both objects being SSOs without associated nebulosity, they may nevertheless be useful as a reference for other bright source observations. No attempt was made for this quick inspection to correct for the object's proper motion. Note that Neptune's brightest moon Triton may reach about 0.5Jy in the blue but should be in the inner part of the PSF at radius $\leq$15arcsec.

It should be noted again that some of the features (ghosts, crosstalk) will show up at different levels, depending on which region of the array and of the instrument was crossed by the source in the particular observation, and how exactly the data were reduced. We illustrate this in Figure 8 using the example of the blue Vesta data already shown above. The left panel shows the map from the psf analysis, using only frames with the source centered within a matrix by some margin and recentering each frame. The middle panel shows a more normal reduction, using all data and (for illustration) a more relaxed deglitching nsigma. Differences between the two images are: (1) the expected slight global shift of the psf core due to the use of recentering or not. (2) the presence of a negative crosstalk signature in the normal processing, because the frames where the source is centered on crosstalking pixels are included, and because deglitching is relaxed enough to let pass these events. (3) a weak diagonal excess emission possibly related to the 'blue streak' ghost feature occuring with the source just outside the corner of the blue array.

Neptune observations confirm the features seen in Vesta. More clearly detected is a dark spot in the +y detection, at a separation differing in blue/green vs red and clearly originating in crosstalk effects (see also PICC-ME-TN-034). Note that the detectability of the spot is a clear function of the deglitching procedure used, like the source itself it may be 'deglitched away' if blindly applying parameters suited for faint source fields.

Very weakly indicated in the Neptune maps are possible linear structures, elongated in z direction and offset by about $\pm$2arcmin in y direction. The reality of these features needs independent confirmation.

The maps of Mars clearly show the 60 degree symmetry multi-spoke pattern expected from the secondary mirror support (see also PICC-ME-TN-029). In both bands, an elongated feature crossing the source in scan direction is observed, likely due to an aftereffect of passing this extremely bright object. Both bands show a weakly elevated structure, roughly rectangular in spacecraft y (array) direction, of unclear origin. The blue map shows clear deglitching artefacts, the red one a crosstalk artefact $\sim$1.7 arcmin to the left of the source that is likely

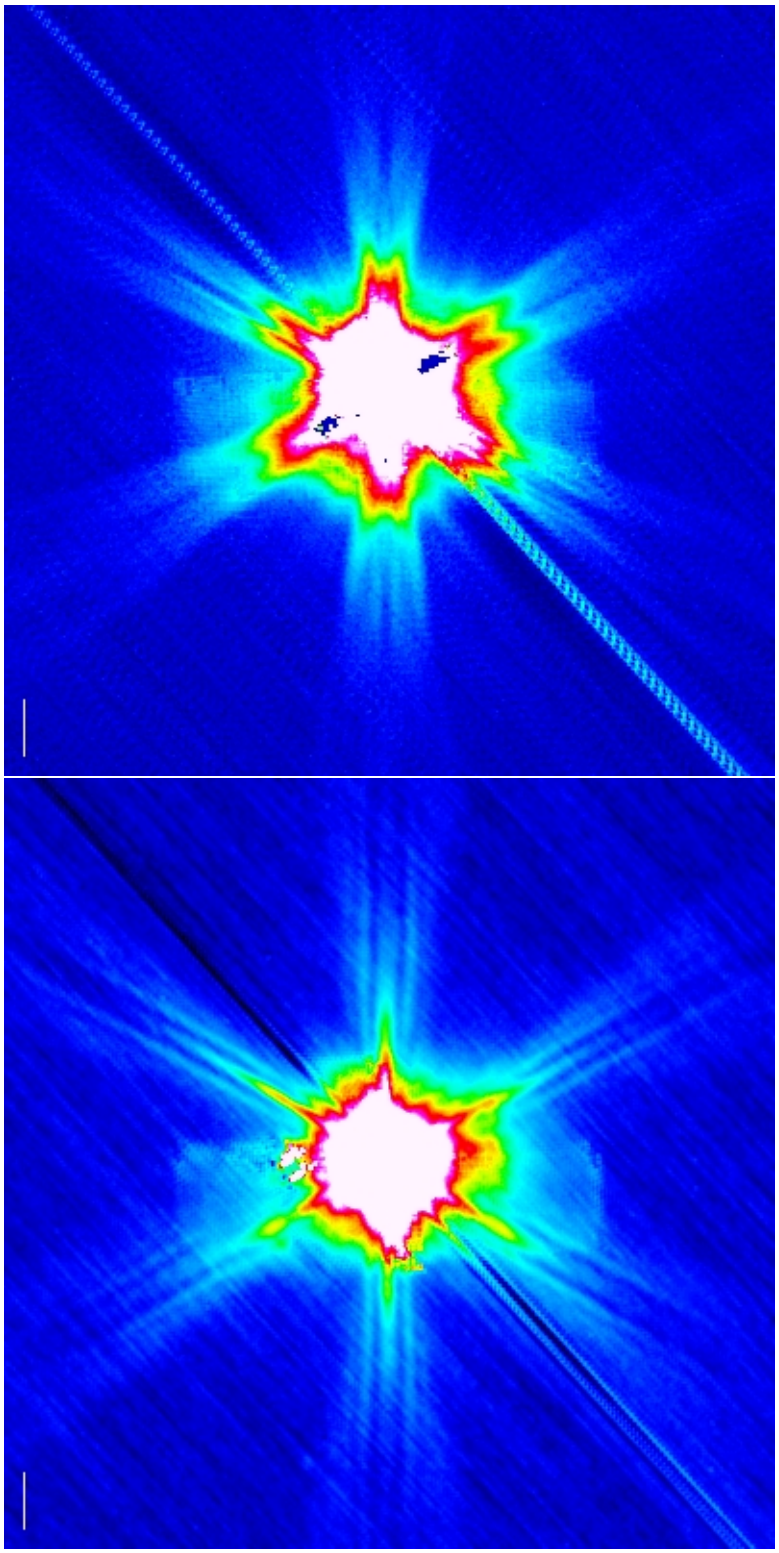

Figure 9: Faint PSF details from scanmaps of Mars, in blue (top) and red (botttom). The scale bar indicates 60arcsec.

further modified by deglitching.

8 Related documents

Review on PACS bolometers time constant, Billot et al., SAp-FIRST-NB-0688-05 (expectations for PSF smearing by fast scan)

PACS Test Analysis Report FM-ILT - Part III PICC-ME-TR-007 Section 3.1.4 (D.Lutz) on Photometer Point Spread Function

Herschel/PACS modelled point-spread functions, N. Geis and D. Lutz, PICC-ME-TN-029

In-orbit crosstalk in the PACS photometer, PICC-ME-TN-034

9 Document change record

Version	Date	Initials	Comment
0.1	2009-09-16	DL	Quick version
0.2	2009-10-27	DL	Added OD160 Vesta
0.3	2009-11-10	DL	Minor updates to Vesta psf, bright source morphology

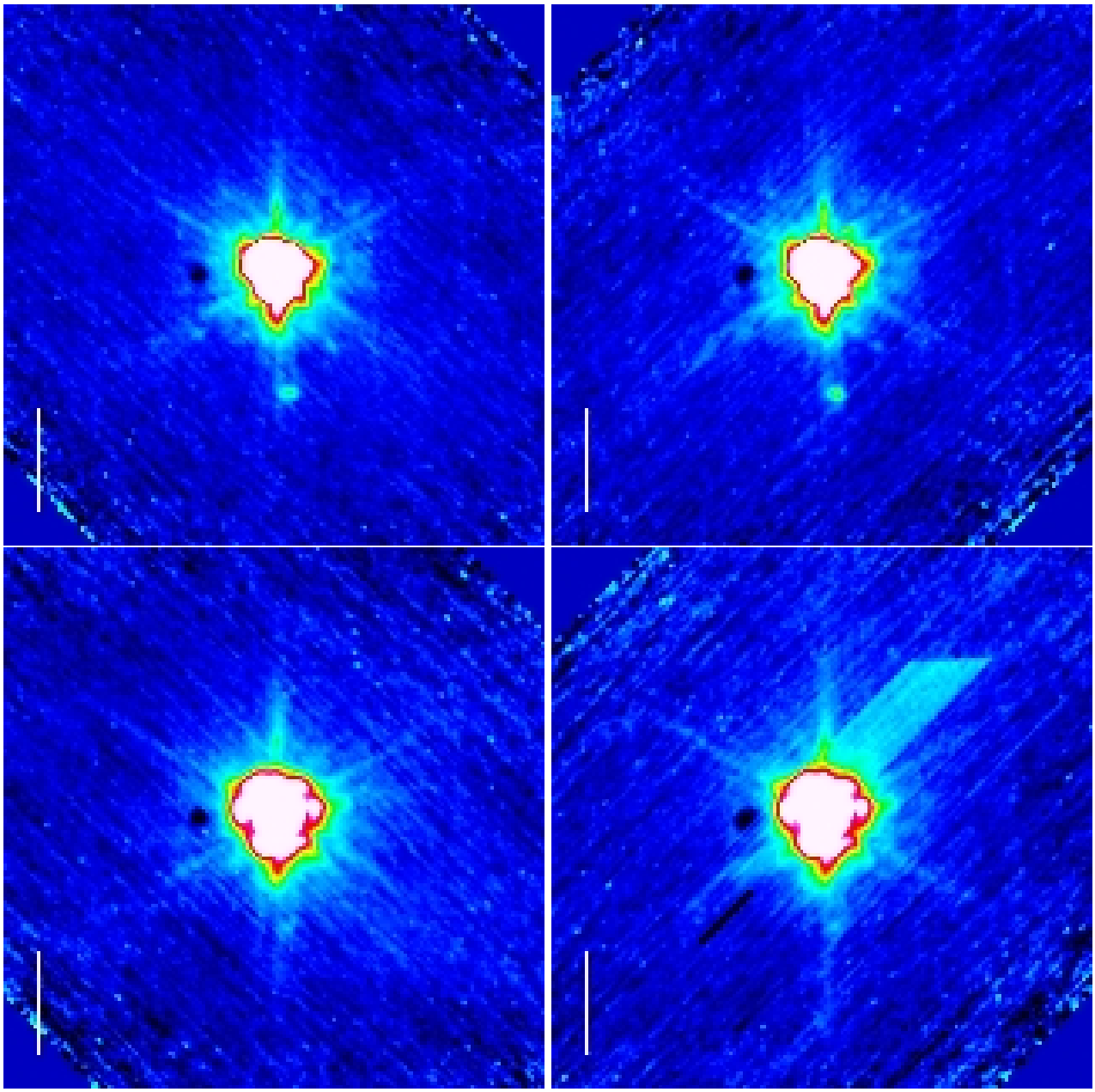

Figure 10: Faint PSF details from scanmaps of Neptune, in blue (top) and green (botttom). The scale bar indicates 60arcsec.

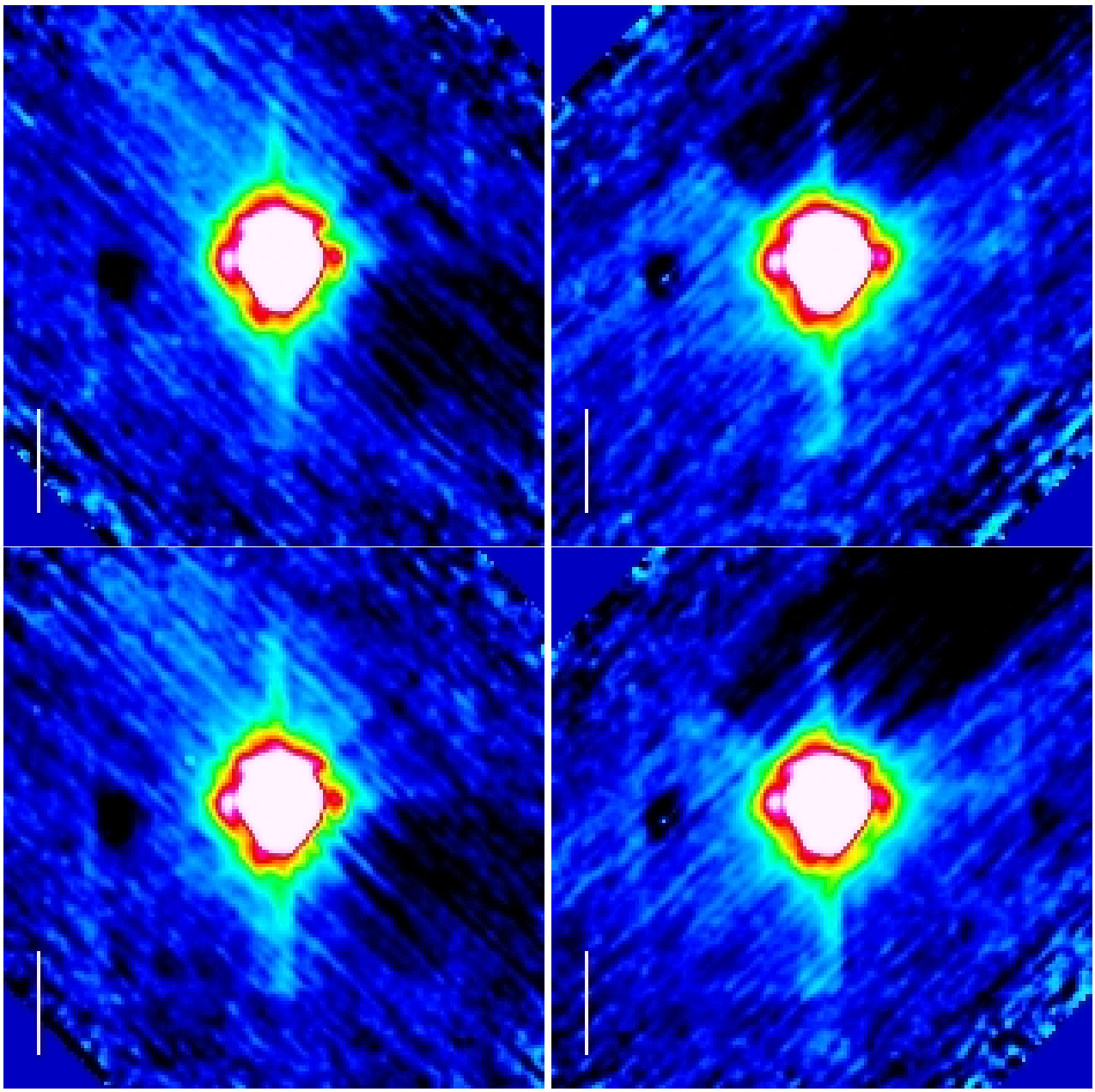

Figure 11: Faint PSF details from scanmaps of Neptune in red. The scale bar indicates 60arcsec.